



## Copyright Notice

©1998 IEEE. Personal use of this material is permitted. However, permission to reprint/republish this material for advertising or promotional purposes or for creating new collective works for resale or redistribution to servers or lists, or to reuse any copyrighted component of this work in other works must be obtained from the IEEE.

This document was downloaded from Chalmers Publication Library (<http://publications.lib.chalmers.se/>), where it is available in accordance with the IEEE PSPB Operations Manual, amended 19 Nov. 2010, Sec. 8.1.9 (<http://www.ieee.org/documents/opsmanual.pdf>)

(Article begins on next page)

# Optimization of Lattices for Quantization

Erik Agrell and Thomas Eriksson

**Abstract**—A training algorithm for the design of lattices for vector quantization is presented. The algorithm uses a steepest descent method to adjust a generator matrix, in the search for a lattice whose Voronoi regions have minimal normalized second moment. The numerical elements of the found generator matrices are interpreted and translated into exact values. Experiments show that the algorithm is stable, in the sense that several independent runs reach equivalent lattices. The obtained lattices reach as low second moments as the best previously reported lattices, or even lower. Specifically, we report lattices in 9 and 10 dimensions with normalized second moments of 0.0716 and 0.0708, respectively, and nonlattice tessellations in 7 and 9 dimensions with 0.0727 and 0.0711, which improves on previously known values. The new 9- and 10-dimensional lattices suggest that Conway and Sloane's conjecture on the duality between the optimal lattices for packing and quantization might be false. A discussion of the application of lattices in vector quantizer design for various sources, uniform and nonuniform, is included.

**Index Terms**—Lattice quantization, normalized second moment, Voronoi region, lattice design, training algorithm.

## I. INTRODUCTION: VECTOR QUANTIZATION AND LATTICES

Lattices are widely recognized as an important tool in the design of vector quantizers, not only for uniform sources. The design can be thought of as two independent problems: the choice of a suitable lattice and the creation of a codebook based on a subset of the lattice. The present paper considers the first of these problems, and the second is studied in, e.g., the report [1].

To select a good lattice, one can of course rely on written sources, such as [2], where many lattices and their properties are tabulated. However, there is reason to believe that the best  $d$ -dimensional lattice has not yet been found for every  $d$  (see, e.g., Fig. 2). Perhaps there is some knowledge to be gained through an approach completely different from the algebraic methods that have been dominating lattice design? This was the question that triggered the present work, and the answer we found was affirmative.

We propose an algorithm for lattice design that can be used with a minimum of insight into algebra and lattice theory. The algorithm employs a numerical algorithm to iteratively improve a given lattice, in a manner that parallels traditional training methods for the design of unconstrained vector quantizers.

This section introduces the background and preliminaries for the work. Section I-A is a brief review of the fundamentals of vector quantization and its terminology. In Section I-B, we then apply

This work was completed while the authors were with the Department of Information Theory, Chalmers University of Technology, Göteborg, Sweden.

E. Agrell is now with the Department of Electrical and Computer Engineering, University of California, San Diego, La Jolla, CA 92093-0407 USA.

T. Eriksson is now with AT&T Labs-Research, Florham Park, NJ 07932-0971 USA.

The material in this paper is based on the report Lattice-Based Quantization, Part I, Tech. report 17, Dept. of Information Theory, Chalmers Univ. of Technology, Göteborg, Sweden, Oct. 1996.

vector quantization to uniform sources, and explain why a lattice is a commonly employed structure of uniform quantizers. After a summary of some lattice theory in Section I-C, we return to the problem of vector quantizer design in Section I-D. This section, which is essentially a literature survey, presents various strategies to design lattice-based vector quantizers for nonuniform sources, which is not as straightforward as in the uniform case.

The lattice training algorithm is presented in Section II. In Section III, experiments with the algorithm are reported, which lead to improvements on previously known results in dimensions 7, 9, and 10. Section IV is a summary.

### A. Vector Quantization

A *vector quantizer* is a general utility for digital representation of multidimensional data. Its input is a real-valued vector  $\mathbf{x}$  and its output is one of a finite number of *codevectors*  $(\mathbf{c}_1, \dots, \mathbf{c}_N)$ , which is selected to approximate  $\mathbf{x}$  as well as possible, according to some criterion. The codevector  $\mathbf{c}_i$  can, through its integer index  $i$ , be represented using  $\log_2 N$  bits. The *rate*  $R$  is the number of bits used to quantize one scalar, that is,  $R = \log_2 N/d$ , where  $d$  is the *dimension* of the quantizer, in other words, the number of components in  $\mathbf{x}$  and  $\mathbf{c}_i$ .

The quantization is governed by a function  $Q: \mathbb{R}^d \rightarrow \mathcal{C}$ , where  $\mathcal{C} = \{\mathbf{c}_1, \dots, \mathbf{c}_N\}$  is the *codebook*. This function should be chosen to optimize some quality measure for a given source. The standard quality measure is the minimum mean square error, or *distortion*, per vector,

$$D = \int_{\mathbb{R}^d} \|\mathbf{x} - Q(\mathbf{x})\|^2 f_{\mathbf{x}}(\mathbf{x}) d\mathbf{x} \quad (1)$$

where  $f_{\mathbf{x}}(\mathbf{x})$  is the probability density function of the source vectors  $\mathbf{x}$ . If the codebook is given, the optimal quantization function is to simply choose the *closest* codevector in the Euclidean sense,

$$Q(\mathbf{x}) = \arg \min_{\mathbf{c} \in \mathcal{C}} \|\mathbf{x} - \mathbf{c}\|^2. \quad (2)$$

This rule reduces the problem of vector quantizer design to finding a point constellation for use as a codebook.

Many input vectors  $\mathbf{x}$  yield the same output vector  $\mathbf{c}_i$ . The set of *all* input vectors that are encoded as the same codevector is called a *Voronoi region*,

$$\Omega_k = \{\mathbf{x} \in \mathbb{R}^d : Q(\mathbf{x}) = \mathbf{c}_k\}. \quad (3)$$

Hence, the function  $Q(\cdot)$  partitions  $d$ -dimensional source space into  $N$  Voronoi regions, without neither gaps nor overlaps. In terms of Voronoi regions, the distortion (1) can be separated into the contributions by each codevector:

$$D = \sum_{i=1}^N \int_{\Omega_i} \|\mathbf{x} - \mathbf{c}_i\|^2 f_{\mathbf{x}}(\mathbf{x}) d\mathbf{x}. \quad (4)$$

In the next section, this expression will be specialized to the case of uniform sources.

The most common way to design a vector quantizer is to generate a large set of source samples, a *training database*, and iteratively adjust ("train") an initial codebook, in order to decrease an estimate of

the distortion, based on the training database. Among the large number of training algorithms that have been proposed, we mention [3],<sup>1</sup> [4], [5, chs. 5 and 7], and [6].

In this paper, an alternative approach for vector quantizer design is studied: lattice-based design. The general idea is to find a lattice with attractive properties and subsequently shape a subset thereof to the source. The focus of this paper is on the lattice itself; truncation and modifications of lattices to suit various sources are discussed in Section I-D.

### B. Quantizer Design for Uniform Sources

This section summarizes the application of vector quantization to uniform sources. Suppose that the source probability density function is uniform within a region  $\Delta$ ,

$$f_{\mathbf{x}}(\mathbf{x}) = \begin{cases} \frac{1}{\text{vol}(\Delta)} & \text{if } \mathbf{x} \in \Delta \\ 0 & \text{if } \mathbf{x} \notin \Delta \end{cases} \quad (5)$$

where  $\text{vol}(\Psi)$  denotes the  $d$ -dimensional volume of a region  $\Psi \subset \mathbb{R}^d$ . Then the distortion (4) becomes

$$D = \frac{1}{\text{vol}(\Delta)} \sum_{i=1}^N \int_{\Omega_i \cap \Delta} \|\mathbf{x} - \mathbf{c}_i\|^2 d\mathbf{x}. \quad (6)$$

Now we concentrate on what happens when the rate  $R$  is high, for a constant dimension  $d$ . The region  $\Delta$  then becomes partitioned into a large number,  $N$ , of Voronoi regions, each one contributing a small amount to the overall distortion  $D$ . According to a well-known conjecture in quantization theory, first posed by Gersho [7], *almost all the Voronoi regions will be similar to each other* in the optimal vector quantizer. In other words, there exists a *typical body* that, through proper scaling, rotation, reflection, and translation, will approximate most of the Voronoi regions.

We will now, supported by Gersho's conjecture, make the approximation that *all* Voronoi regions are congruent to a typical body  $\Omega_t$ . Moreover, since the source under consideration is uniform, we assume that all regions have the same size. Hence, the Voronoi regions are translations (possibly rotated or reflected) of  $\alpha\Omega_t$ ,<sup>2</sup> where  $\alpha$  is a rate-dependent scaling parameter to be determined below. This approximation contains two errors, for any finite rate. Firstly, the regions in (6) deviate a little from  $\alpha\Omega_t$ ; secondly, some of the regions, notably those close to the boundary of  $\Delta$ , deviate a lot. How these errors are handled implicitly selects one of two concepts for vector quantizer design for uniform sources. The errors can be neglected, which is the basic assumption behind lattice quantization, or they can be considered, which leads into unconstrained quantizer design. In this paper, we follow the former approach.

If all Voronoi regions are congruent, the sum in (6) is not needed anymore:

$$\begin{aligned} D &\approx \frac{1}{\text{vol}(\Delta)} N \int_{\alpha\Omega_t} \|\mathbf{x} - \alpha\mathbf{c}_t\|^2 d\mathbf{x} \\ &= \frac{1}{\text{vol}(\Delta)} N \int_{\Omega_t} \|\alpha\mathbf{y} - \alpha\mathbf{c}_t\|^2 \alpha^d d\mathbf{y}. \end{aligned} \quad (7)$$

The value of  $\alpha$  as a function of  $N$  can be deduced by considering the total volume that the regions cover. The volume is

$$\text{vol}(\Delta) \approx N \text{vol}(\alpha\Omega_t) = N\alpha^d \text{vol}(\Omega_t) \quad (8)$$

from which follows that

$$\alpha \approx \left( \frac{\text{vol}(\Delta)}{N \text{vol}(\Omega_t)} \right)^{1/d}. \quad (9)$$

This value inserted into (7) yields

$$\begin{aligned} D &\approx \left( \frac{\text{vol}(\Delta)}{N} \right)^{2/d} \left( \frac{1}{\text{vol}(\Omega_t)} \right)^{1+2/d} \int_{\Omega_t} \|\mathbf{y} - \mathbf{c}_t\|^2 d\mathbf{y} \\ &= d \text{vol}(\Delta)^{2/d} 2^{-2R} G \end{aligned} \quad (10)$$

where

$$G = \frac{1}{d \text{vol}(\Omega_t)^{1+2/d}} \int_{\Omega_t} \|\mathbf{y} - \mathbf{c}_t\|^2 d\mathbf{y} \quad (11)$$

is the *normalized second moment* of the typical body  $\Omega_t$ . This measure is independent of the rate and the source shape. It is also dimensionless and thus insensitive to scaling. Hence, congruent bodies have the same  $G$ . The normalization with respect to  $d$  is to make easier the comparison between quantizers of different dimensions. This paper is devoted to the search for structures with a low value of  $G$ .

The distortion expression (10) can be used to estimate the performance of a well-optimized high-rate vector quantizer for a uniform source. Conversely, it can also be used as a tool in the design of such quantizers. The method is to find a  $d$ -dimensional body  $\Omega_t$  with a low  $G$ . Every body is not admissible; only bodies that can form a *tessellation*. A tessellation is a partition of  $\mathbb{R}^d$  into regions, such that any pair of regions can be transformed into each other through rotation, reflection, and translation.<sup>3</sup> When a tessellation is found that consists of bodies with a low  $G$ , the codebook is formed as the intersection of the centroids and  $\Delta$ . The desired rate determines the scaling of the tessellation. The structure is called a *tessellating quantizer* [8]. In previous studies of tessellating quantizers, most attention has been devoted to *lattice quantizers*, which constitute an important subset of all tessellation quantizers. Lattices are defined in the next section.

### C. Lattices

A *lattice* is a popular special case of a tessellation.<sup>4</sup> The following brief summary of lattice theory is intended to be a sufficient background for the quantization problem investigated in this paper. For a more extensive treatment, the interested reader is referred to the book by Conway and Sloane [2], which has more or less become the standard textbook on lattice theory.

A lattice is an infinite set of vectors, defined through  $d$  linearly independent *basis vectors*  $\mathbf{b}_1, \mathbf{b}_2, \dots, \mathbf{b}_d$ . The lattice consists of all linear combinations of the basis vectors, with integer coefficients. The matrix whose rows are the basis vectors is called the *generator matrix* of the lattice,

$$\mathbf{B} = [\mathbf{b}_1, \mathbf{b}_2, \dots, \mathbf{b}_d]^T. \quad (12)$$

Formally, we can write the lattice  $\Lambda$  as

<sup>1</sup> Lloyds original manuscript, which although unpublished has become famous, is dated 1957.

<sup>2</sup> We will allow the following operation on a set  $\Psi$  of vectors: Elementwise multiplication by a scalar  $a$ , denoted  $a\Psi$ , and elementwise addition of a vector  $\mathbf{a}$ , denoted  $\Psi + \mathbf{a}$ .

<sup>3</sup> The body with the lowest  $G$  is the  $d$ -dimensional sphere, but it is not admissible as  $\Omega_t$ , because it cannot form a tessellation (for  $d \geq 2$ ).

<sup>4</sup> With a slight abuse of terminology, we will use "tessellation" to denote both a partition of the type defined above and an infinite set of points whose Voronoi regions form such a partition.

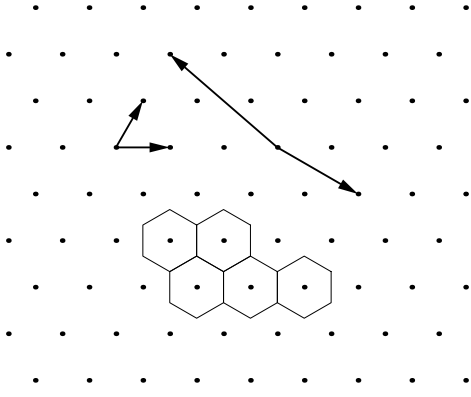


Fig. 1. Two possible bases for the hexagonal lattice. Some of the Voronoi regions are shown.

$$\Lambda = \{ \mathbf{x} \in \mathbb{R}^d : (\mathbf{B}^{-1})^T \mathbf{x} \in \mathbb{Z}^d \}. \quad (13)$$

Hence, any lattice point<sup>5</sup> can be uniquely written as  $\mathbf{B}^T \mathbf{u}$ , where  $\mathbf{u} \in \mathbb{Z}^d$ .

Fig. 1 is an example of a lattice. It is the well-known hexagonal lattice, also called  $A_2$ , and can be defined through, e.g., the generator matrix

$$\begin{bmatrix} 2 & 0 \\ 1 & \sqrt{3} \end{bmatrix}. \quad (14)$$

$A_2$  is the 2-dimensional case of the lattice  $A_d$ , which is defined, along with some other common lattices, in the appendix.

In the design and analysis of lattices, it is often convenient to employ  $d$  basis vectors having more than  $d$  coordinates. However, throughout this paper,  $\mathbf{B}$  denotes a square generator matrix. This notation does not restrict generality, since  $d$  vectors cannot span more than  $d$  dimensions. Hence, for every nonsquare generator matrix  $\mathbf{B}'$ , there exists a square matrix  $\mathbf{B}$  describing an *equivalent* lattice. (More on equivalent lattices below.) Practically, such a  $\mathbf{B}$  can be found through, e.g., QR factorization of  $(\mathbf{B}')^T$  or Cholesky decomposition of  $\mathbf{B}'(\mathbf{B}')^T$ . Some of the following theory draws advantage of  $\mathbf{B}$  being square, thus simplifying the notation. For example, both the inverse and the determinant of  $\mathbf{B}$  have important interpretations.

Lattice points are evenly distributed in space—there is no region where the lattice is denser than somewhere else. It is because of this uniformity that lattices are suitable for the quantization of uniform sources. Gersho pointed out, “if you sit on one lattice point and view the surrounding set of lattice points, you will see the identical environment regardless of which point you are sitting on” [9]. Consequently, the Voronoi regions form a tessellation, as mentioned above in Section I-B. Indeed, the Voronoi regions are pure translations of each other, without needing any rotation or reflection. (See Fig. 1 for an example.) This is a chief characteristic of all lattices.

The all-zero vector  $\mathbf{0}$  belongs to all lattices. This follows trivially from the definition (13). The Voronoi region around  $\mathbf{0}$ ,

$$\Omega = \{ \mathbf{x} \in \mathbb{R}^d : \|\mathbf{x}\|^2 \leq \|\mathbf{x} - \mathbf{c}\|^2 \text{ for all } \mathbf{c} \in \Lambda \}, \quad (15)$$

is commonly called *the* Voronoi region of the lattice  $\Lambda$ . It is the standard choice of a typical body (see Section I-B) in the computation of lattice parameters. The volume of  $\Omega$  is  $V = \text{vol}(\Omega) = |\det \mathbf{B}|$ .<sup>6</sup> The normalized second moment (11) is

<sup>5</sup> We use “lattice point” and “lattice vector” interchangeably.

<sup>6</sup> The volume is more commonly given in the form  $(\det(\mathbf{B}\mathbf{B}^T))^{1/2}$ , which allows for nonsquare generator matrices.

$$G = \frac{1}{dV^{1+2/d}} \int_{\Omega} \|\mathbf{x}\|^2 d\mathbf{x}. \quad (16)$$

A complication in the analysis of lattices is that equivalent lattices can be specified through seemingly different generator matrices. Two lattices are considered *equivalent* if their Voronoi regions (15) are congruent. In this case, the two lattices have the same  $G$ , and most other lattice parameters agree, too. For example, the generator matrices

$$\begin{bmatrix} -2 & 0 \\ 3 & 1/\sqrt{3} \end{bmatrix}, \begin{bmatrix} \sqrt{3}+1 & \sqrt{3}-1 \\ \sqrt{3}-1 & \sqrt{3}+1 \end{bmatrix}, \text{ and } \begin{bmatrix} 2-\pi\sqrt{2} & 2-\pi\sqrt{2} \\ 1-1/\sqrt{3}+\pi/\sqrt{6} & 1+1/\sqrt{3}-\pi/\sqrt{2} \end{bmatrix}$$

all specify the  $A_2$  lattice, so these lattices are equivalent to the one given by (14).

A lattice can be transformed by scaling, rotation, and reflection, without changing the shape of the Voronoi region.<sup>7</sup> In addition, basis vectors can be selected in many ways within the point set  $\Lambda$ , as illustrated in Fig. 1. It can be shown that the lattices generated by  $\mathbf{B}_1$  and  $\mathbf{B}_2$  are equivalent if and only if there exist matrices  $\mathbf{W}$  and  $\mathbf{Q}$  such that

$$\mathbf{B}_2 = \left( \frac{V_2}{V_1} \right)^{1/d} \mathbf{W} \mathbf{B}_1 \mathbf{Q} \quad (17)$$

where all elements of  $\mathbf{W}$  are integers,  $\mathbf{W}$  has determinant  $\pm 1$ , and  $\mathbf{Q}$  is orthonormal. The coefficient  $(V_2/V_1)^{1/d}$  takes care of scaling,  $\mathbf{W}$  of basis change, and  $\mathbf{Q}$  of rotation and/or reflection. Unfortunately, there has, to our best knowledge, not been published any general algorithm to determine whether two given generator matrices specify equivalent lattices. Of course, if either  $\mathbf{W}$  or  $\mathbf{Q}$  is known, the other one is obtained by matrix inversion, but to determine both of them simultaneously is still an open problem. It has been suggested to employ a *canonical form* for lattices to solve the problem: if  $\mathbf{B}_1$  and  $\mathbf{B}_2$  have the same canonical form, they are equivalent; otherwise not. Unfortunately, the algorithms that have been proposed to transform a generator matrix into a canonical form (see, e.g., [10, pp. 65–67] and [11, pp. 184–201]) consider basis changes only, not rotation. If  $\mathbf{B}_1$  and  $\mathbf{B}_2$  are rotated versions of the same lattice, the canonical forms obtained by such an algorithm will differ. Hence, the problem of identifying equivalent lattices remains, as discussed in Section II-C.

Finally, for every lattice there is a *dual*. The dual of  $\Lambda$  is another lattice, whose generator matrix is  $(\mathbf{B}^{-1})^T$ . The dual is denoted  $\Lambda^*$ . It has the same degree of symmetry as  $\Lambda$ , but the lattice parameters, such as the normalized second moment  $G$ , are normally different.

#### D. Quantizer Design for Nonuniform Sources

We now return to vector quantization. So far, the discussion has been focused upon uniform sources, where lattices are immediately applicable as quantizer structures. While under some circumstances, for example, image data can be modeled as a uniform source [12, p. 33], most applications display different probability density functions. However, lattices have found their use in vector quantization for nonuniform sources, too.<sup>8</sup> In this section, we will review some approaches that have been proposed in the past.

One possibility is, of course, to approximate the probability density function of the source with a uniform function, and design a

<sup>7</sup> Translation also preserves the Voronoi region, but a translated lattice is normally not a lattice (13). It is still, of course, a tessellation.

<sup>8</sup> In fact, all applications of lattices that are mentioned in this section are directly generalizable to other types of tessellations as well. We retain the lattice terminology because it is the framework in which most of the research was originally published.

*lattice quantizer* (Section I-B) accordingly. Much attention has been devoted to the problem of optimizing the size and shape of the uniform function for a given source density; in other words, the problem of scaling and truncation of the lattice. This problem is discussed in [1] and several of its references. The gain in memory and encoding time, compared with a source-optimized codebook, is significant. The price paid is a performance degradation, the severity of which depends on the rate, the dimension, and the probability density of the source. The general trend is that the degradation increases with higher rate and lower dimension, as illustrated for a Gaussian source in Fig. 3.4 of [1].

For high-dimensional sources, a low-rate lattice quantizer is known to have close to optimal performance. This is because of the *asymptotical equipartition property*, according to which a large class of high-dimensional probability density functions can be well approximated with uniform densities [13, pp. 73, 285], [14]. For example, data drawn from an uncorrelated Gaussian density tend to be uniformly distributed in a thin spherical shell, if the dimension is high [15], whereas the multidimensional Laplacian density can be approximated by a uniform density on the surface of a “pyramid” (hyperoctahedron) [16]. The tendency towards uniform distributions has been successfully employed in several applications. Competitive lattice quantizers have been designed for use in CELP [17] and transform coded [18] speech coding systems. In image coding, Jeong and Gibson have achieved good performance through lattice quantized DCT coefficients [19]. For high rates and low dimensions, on the other hand, the performance degradation of lattice quantizers compared with source-optimized vector quantizers can be quite severe [20, 21, 1].

To avoid performance degradation due to nonuniform sources, the quantizer should be matched to the specific source density, but still there exist promising alternatives to the training of an unconstrained codebook. The basic idea is to maintain the local lattice-similarity while making the global structure matched to the source.

One quantizer structure with this aim is the *piecewise uniform* quantizer introduced by Kuhlmann and Bucklew [22, 20]. It is a generalization of the lattice quantizer, where a given (nonuniform) probability density function is approximated with a staircase function. In each region where the density approximation is constant, the codebook is populated by a suitably scaled lattice. Similar structures are obtained by designing two-stage quantizers where the second stage is a lattice [23, 24, 25].

A more general method to improve the performance of a lattice quantizer for nonuniform source densities is to apply a nonlinear transform function to each input vector before quantization, and the inverse function to quantized data. This approach is called *companding* and it is used in many scalar applications. It was suggested for use in vector quantization by Gersho [7], and Bucklew characterized its high-rate performance [26, 27]. Antonini et al. applied companding and lattice vector quantization to wavelet coefficients for image data [28]. The piecewise uniform quantizer is a special case of a companding lattice quantizer, where the transform function is piecewise linear.

An alternative method to modify a lattice quantizer to match a nonuniform source is presented in [1], where the advantages of a lattice structure are incorporated into a design algorithm for source-optimized vector quantizers.

In Section I-A it was assumed that each codevector was encoded with exactly  $\log_2 N$  bits. If the codevectors have unequal *a priori* probabilities, the average rate can be reduced by applying an entropy

code to the quantizer output. It has been shown that if an entropy code is employed, the *optimal high-rate vector quantizer should have a uniform distribution of codevectors* [7] [29, p. 131] [30, p. 471]. Hence, if Gersho’s conjecture (see Section I-B) is true, then a tessellating quantizer is asymptotically optimal when the rate tends to infinity. The optimality does not require the source density to be uniform or even smooth, only that the differential entropy is finite, as proved by Linder and Zeger [8]. It is worth mentioning that a tessellating quantizer with entropy coding performs closer to the rate-distortion bound than the optimal fixed-rate vector quantizer. The argument behind this statement is the following: The optimal fixed-rate vector quantizer is inferior to (has higher average rate than) the same quantizer with an entropy code. And a codebook with nonuniform point density is inferior to a uniform codebook, as long as entropy coding is being applied. Applications of entropy coded lattice quantization are presented in, e.g., [14, 31, 32].

For high rates, the performance of an entropy-coded tessellating quantizer is proportional to the normalized second moment  $G$  of the tessellation. This was shown in [8], through the high-rate approximation

$$D \approx dG2^{2(h-H)/d} \quad (18)$$

in which  $h = \int f_x(\mathbf{x}) \log_2 f_x(\mathbf{x}) d\mathbf{x}$  is the differential entropy of the source and  $H$  is the output entropy of the quantizer,  $H = -\sum p_i \log_2 p_i$ , where  $p_i$  is the probability of the event  $Q(\mathbf{x}) = \mathbf{c}_i$ . The approximation is asymptotically exact, in the sense that the relative error tends to zero as  $H$  approaches infinity. The factor  $G$  in (18) shows the importance of tessellations with a low  $G$ ; the gain obtained by improving a tessellation can be expected to propagate directly into the distortion of an entropy-coded quantizer built upon the tessellation. A distortion proportional to  $G$  is also a feature of, e.g., high-rate uniform quantization (10), nonuniform quantization [33], and lattice quantization of Gaussian sources [21] [1, sec. 3.2].

Hence, we turn our attention towards the minimization of  $G$ .

## II. NUMERICAL OPTIMIZATION OF LATTICES

The history of lattice design is closely interlinked with group theory and error-correcting codes. Almost all lattice design methods that have been proposed arise from the algebraic approach. We now study an alternative method. The idea to iteratively adjust a lattice in order to decrease the normalized second moment was suggested in [34], but to the best of our knowledge, no specific algorithm for the purpose has yet been presented.<sup>9</sup> We have developed an algorithm that minimizes the normalized second moment by a gradient search procedure. The algorithm is related to algorithms for vector quantizer training, but it operates on a generator matrix instead of individual codevectors. In Section II-A, we regard lattice design for quantization as an optimization problem and adopt a suitable set of variables. The new algorithm is presented in detail in Section II-B, together with the theoretical background. Section II-C discusses in general terms what kind of results is expected from the algorithm, and how these results can be interpreted.

### A. The Optimization Problem

The problem of finding a good lattice for high-rate uniform quantization can be stated as a multivariate minimization problem

<sup>9</sup> For the design of binary codes, however, iterative algorithms have been employed, see [35] and its references.

$$\min_{\mathbf{B} \in \mathbb{R}^{d \times d}} G \quad (19)$$

where  $G$  is the normalized second moment (16)

$$G = \frac{1}{dV^{1+2/d}} \int_{\Omega} \|\mathbf{e}\|^2 d\mathbf{e}. \quad (20)$$

The problem contains  $d^2$  unknowns, or degrees of freedom, namely, the  $d^2$  elements of the generator matrix, which specify the lattice through the construction (13).

To simplify the problem, we recall the concept of equivalent lattices, see Section I-C, especially (17). There are many ways to change a generator matrix into one that spans an equivalent lattice, and such changes do not affect the normalized second moment  $G$  at all. On the contrary, an iterative optimization algorithm should concentrate on changes that has a potential of improving the lattice. Why attempt a 100-variate optimization problem when 50 variables suffice? If we fix the rotation of the lattice, and the scaling, almost half of the  $d^2$  variables in the generator matrix can be removed from the minimization. Specifically, the rotation is in (17) controlled by an orthonormal  $d \times d$  matrix, and the set of all such matrices spans a parameter space of  $d(d-1)/2$  dimensions. This number of variables disappear from the minimization problem when the rotation is fixed; one more variable disappears when the scale factor is fixed.<sup>10</sup> Hence, of the  $d^2$  degrees of freedom that a general generator matrix  $\mathbf{B}$  possesses,  $d(d-1)/2 + 1$  are irrelevant in the optimization of  $G$ , whereas  $d^2 - d(d-1)/2 - 1 = (d+2)(d-1)/2$  are important. The irrelevant degrees of freedom can be removed from the generator matrix in several ways; we employ the following straightforward method.

Using (17), it is easily shown that for any lattice, there exists an equivalent lattice with a generator matrix of the form

$$\mathbf{B} = \begin{bmatrix} b_{1,1} & 0 & \cdots & 0 & 0 \\ b_{2,1} & b_{2,2} & \cdots & 0 & 0 \\ \vdots & \vdots & & \vdots & \vdots \\ b_{d-1,1} & b_{d-1,2} & \cdots & b_{d-1,d-1} & 0 \\ b_{d,1} & b_{d,2} & \cdots & b_{d,d-1} & \prod_{k=1}^{d-1} b_{k,k}^{-1} \end{bmatrix}. \quad (21)$$

Geometrically, this form locks the first basis vector,  $\mathbf{b}_1$ , along the first axis of the coordinate system,  $\mathbf{b}_2$  in the plane spanned by the first two axes, etc. In addition, the volume of the Voronoi regions,  $V$ , is locked to unity. The training algorithm to be presented in the next section operates on a matrix of the type (21). The matrix can be regarded as a function of

$$\mathbf{f} = (f_1, \dots, f_{(d+2)(d-1)/2})^T \quad (22)$$

where

$$f_{i(i-1)/2+j} = b_{i,j} \quad \text{for } j=1, \dots, d-1 \text{ and } i=j, \dots, d \quad (23)$$

are the  $(d+2)(d-1)/2$  ‘‘free’’ variables in the optimization.

The constraint thus imposed on the form of the generator matrix  $\mathbf{B}$  actually serves two purposes in the simplification of the numerical optimization problem (19). The number of variables are reduced, as discussed above, and it is also worth observing that the objective function itself (20) gets a simpler form, namely,

$$G = \frac{1}{d} \int_{\Omega} \|\mathbf{e}\|^2 d\mathbf{e} \quad (24)$$

<sup>10</sup> The change of basis vectors, as denoted by the matrix  $\mathbf{W}$  in (17), does not contribute any degrees of freedom in the sense discussed here, since the elements of  $\mathbf{W}$  are subject to an integer constraint.

because of the volume normalization. This expression contains no determinant, which will lead to a very simple form for the gradient derived in the next section.

### B. The Lattice Training Algorithm

The training of a lattice basis is in many ways similar to training of an unstructured VQ for a uniform probability density function, but there are also important differences. For instance, the centroid condition for local optimality of a VQ [30, sec. 11.2] is of no help, since the codevectors of *any* lattice are the centroids of their Voronoi regions. This means that we cannot use the generalized Lloyd algorithm in its common form, or, for that matter, any other algorithm that relies on the centroid condition, for the training. We propose a steepest descent algorithm, which is found to be reliable and sufficient for the problems considered here. In higher dimensions, it might be rewarding to study more sophisticated algorithms, such as the Gauss-Newton method and its relatives.

In the development of the algorithm, we take advantage of the problem formulation in the previous section. The strategy is to iterate the vector  $\mathbf{f}$  (22) in order to decrease  $G$  (24). Random training vectors are generated with a uniform distribution inside the Voronoi region  $\Omega$ . For each training vector, the squared distance to the origin is computed, and also the gradient of the squared distance with respect to  $\mathbf{f}$ . Then  $\mathbf{f}$ , and thus the generator matrix, is adjusted a small step in the direction of the negative gradient. The adjustment can be made for each individual training vector or for blocks of vectors.

The first question is how to generate the training vectors. Conway and Sloane give an elegant method to generate uniform data within a Voronoi region [36]. First,  $d$  independent random numbers are obtained, uniformly distributed between 0 and 1. They constitute a random vector within the  $d$ -dimensional unit cube. Calling this vector  $\mathbf{z}$ , another vector  $\mathbf{x} = \mathbf{B}^T \mathbf{z}$  is created. Next, a search algorithm is applied to find the closest codevector to  $\mathbf{x}$  in the lattice, denoted  $\mathbf{c}^* = \mathbf{B}^T \mathbf{u}$ . Finally, the difference vector  $\mathbf{e} = \mathbf{x} - \mathbf{c}^*$ , which has a uniform distribution over the Voronoi region  $\Omega$ , is computed.

To steer the training, we need the gradient of the integrand in (24). Hence, we differentiate  $\|\mathbf{e}\|^2$  with respect to each component of  $\mathbf{f}$ :

$$\frac{\partial \|\mathbf{e}\|^2}{\partial b_{i,j}} = \frac{\partial}{\partial b_{i,j}} \sum_{k=1}^d e_k^2 = 2 \sum_{k=1}^d e_k \cdot \frac{\partial e_k}{\partial b_{i,j}} \quad (25)$$

where  $e_k$  denotes component  $k$  of  $\mathbf{e}$ . To find the partial derivatives  $\partial e_k / \partial b_{i,j}$ ,  $\mathbf{e}$  is first written as a function of  $\mathbf{f}$ . Defining  $\mathbf{y} = (y_1, \dots, y_d) = \mathbf{z} - \mathbf{u}$ , we obtain

$$\mathbf{e} = \mathbf{x} - \mathbf{c}^* = \mathbf{B}^T \mathbf{z} - \mathbf{B}^T \mathbf{u} = \mathbf{B}^T \mathbf{y} \quad (26)$$

or, componentwise,

$$e_k = \sum_{l=1}^d b_{l,k} y_l. \quad (27)$$

This gives  $\mathbf{e}$  as a function of  $\mathbf{B}$ , which in turn is a function of  $\mathbf{f}$ . To continue, we employ (21):

$$\begin{aligned} e_k &= \sum_{l=k}^d b_{l,k} y_l \\ &= \begin{cases} \sum_{l=k}^d b_{l,k} y_l & \text{if } k < d \\ y_d \prod_{l=1}^{d-1} b_{l,l}^{-1} & \text{if } k = d \end{cases} \end{aligned} \quad (28)$$

which is a function of  $\mathbf{f}$  only. The derivative is

$$\frac{\partial e_k}{\partial b_{i,j}} = \begin{cases} y_i & \text{if } j = k < d \\ -\frac{y_d}{b_{i,i}} \prod_{l=1}^{d-1} b_{l,i}^{-1} & \text{if } i = j \text{ and } k = d. \\ 0 & \text{otherwise} \end{cases} \quad (29)$$

Inserted into (25), finally, this yields

$$\frac{\partial \|\mathbf{e}\|^2}{\partial b_{i,j}} = \begin{cases} 2e_j y_i & \text{if } i \neq j \\ 2e_i y_i - \frac{2e_d y_d}{b_{i,i}} \prod_{l=1}^{d-1} b_{l,i}^{-1} & \text{if } i = j \end{cases} \quad (30)$$

for all components  $b_{i,j}$  of  $\mathbf{f}$ . Equation (30) gives, componentwise, the gradient of  $\|\mathbf{e}\|^2$  with respect to  $\mathbf{f}$ . According to the steepest descent rule,  $\mathbf{f}$  should be updated in the direction of the negative gradient.

Many small changes to a matrix may eventually make it ill-conditioned. This means that an iterative algorithm for lattice design may grow long and almost parallel basis vectors, which may slow the algorithm down and in severe cases cause numerical problems. For instance, such basis matrices tend to generate ‘‘sensitive’’ lattices, in the sense that a small change of an element yields a large change in the normalized second moment  $G$ . Sensitive lattices could potentially prevent the algorithm from converging, at least if they would be present near a local minimum.

Fortunately, there is a way to counteract this problem. Again we rely on the theory of equivalent lattices. Through a basis change, a given generator matrix can be replaced by one in which the basis vectors are short and reasonably orthogonal to each other. This process, which is called reduction, should be repeated regularly during lattice training. Several reduction algorithms have been proposed, of which the one by Lenstra et al. [37] is probably the

most popular. The reduction normally destroys the triangular structure of the generator matrix, so reduction is immediately succeeded by rotation in our algorithm. It is worth stressing that neither reduction nor rotation changes the lattice (except into an equivalent one); it is the representation of the lattice that is changed.

Some details must be decided in order to complete the training algorithm. The choices include block- or sample-iterative training, step size values, etc. In Table I, we have formulated one suggestion, a sample-iterative algorithm with linearly decreasing step size. Note that the diagonal elements of the generator matrix are updated differently from the other elements. The upper triangular part is not updated, and the last diagonal element,  $b_{d,d}$ , is computed from the other diagonal components as in (21). In the execution of the training algorithm, we employ  $b_{d,d}$  to simplify the expressions (28) and (30). Still,  $b_{d,d}$  should be regarded purely as a function of other matrix elements, and  $b_{d,d}$  does not enter the vector of optimization variables,  $\mathbf{f}$ .

Any lattice can serve as initial value for  $\mathbf{B}$ . We recommend the cubic lattice (see appendix), possibly with a small random disturbance. This lattice is neutral, in the sense that it is not close to any local optimum. Almost any adjustment will reduce the normalized second moment. Metaphorically speaking, the cubic lattice lies on top of the hill. Of course, a better lattice can be used as initialization, if the user wishes to examine this specific lattice, for instance to determine whether it is a local optimum, but this is not a good strategy in the search for a global optimum, especially if the chosen initial lattice is already good. From a point below the hill, you will not see the deep valleys on the other side. The strength of our training algorithm is that it may point at previously unknown lattices.

Three training parameters,  $\epsilon_0$ ,  $M$ , and  $M_r$ , must be specified in advance for the algorithm. Our standard choice, empirically found, is  $\epsilon_0 = 10^{-3}$ ,  $M = 10^7$ , and  $M_r = 10^4$ . Small changes in the values, tailored to the intended experiment, may yield slightly improved performance (in terms of speed and/or quality), but the algorithm is not too sensitive to these parameter values. In fact,  $M_r = \infty$  works well in dimensions up to about 10, which means that low-dimensional lattices can be designed by a simplified version of the algorithm, in which step 5 is omitted.

The computational complexity in the training algorithm is, for high  $d$ , dominated by the so-called *closest point problem*, the search for the closest lattice point of the training data, in step 3. Algorithms have been developed by Kannan [38] and Agrell and Eriksson [39]. It has been theoretically proved that the problem is NP-hard, see, e.g., [40], but the complexity is nevertheless not overwhelming. To indicate the order of magnitude, we mention that with one implementation of the algorithm in [39], the average time to find the closest point in a 24-dimensional lattice is 37 milliseconds.

The lattice training algorithm is easily modified to solve other problems that can be formulated in a similar framework. For example, if we search for a lattice under the constraint of a specific structure, all that is needed is the identification of a vector of free optimization variables  $\mathbf{f}$  and the gradient of  $\|\mathbf{e}\|^2$  with respect to this vector. One application of this idea is reported in Section III-B, where the generator matrix (31) was refined by such a constrained lattice training algorithm.

### C. Identification of Lattices

In applications of numerical optimization, exact solutions cannot be expected. The presented training algorithm for lattices is of course no exception: the results are approximations of true optima, local or

TABLE I  
THE LATTICE TRAINING ALGORITHM.

<p><b>Step 1:</b> Initialize a generator matrix <math>\mathbf{B}</math> of the form (21). Set the number of iterations <math>M</math>, the start step size <math>\epsilon_0</math>, and the reduction interval <math>M_r</math> to suitable values. Set <math>m = 1</math>.</p> <p><b>Step 2:</b> Compute a new training vector as <math>\mathbf{x} = \mathbf{B}^T \mathbf{z}</math>, where each component of <math>\mathbf{z}</math> is uniformly distributed in the interval (0,1).</p> <p><b>Step 3:</b> Find the lattice vector <math>\mathbf{c}^* = \mathbf{B}^T \mathbf{u}</math> that is closest to the training vector <math>\mathbf{x}</math>. Set <math>\mathbf{y} = \mathbf{z} - \mathbf{u}</math> and <math>\mathbf{e} = \mathbf{B}^T \mathbf{y}</math>.</p> <p><b>Step 4:</b> Update the components of <math>\mathbf{B}</math> for <math>j = 1, \dots, d-1</math> and <math>i = j, \dots, d</math> as</p> $b_{i,j} := b_{i,j} - \epsilon_m \cdot \frac{\partial \ \mathbf{e}\ ^2}{\partial b_{i,j}}$ <p>where</p> $\frac{\partial \ \mathbf{e}\ ^2}{\partial b_{i,j}} = \begin{cases} 2e_j y_i & \text{if } i \neq j \\ 2e_i y_i - 2e_d y_d \frac{b_{d,d}}{b_{i,i}} & \text{if } i = j \end{cases}$ <p>and <math>\epsilon_m</math> is a linearly decreasing step size parameter, <math>\epsilon_m = \epsilon_0(1 - m/M)</math>. The last diagonal element, <math>b_{d,d}</math>, is computed by the expression</p> $b_{d,d} = \left( \prod_{k=1}^{d-1} b_{k,k} \right)^{-1}$ <p><b>Step 5:</b> If <math>m</math> is divisible by <math>M_r</math>, then perform a reduction on <math>\mathbf{B}</math> and subsequently rotate <math>\mathbf{B}</math> into lower triangular form.</p> <p><b>Step 6:</b> If the desired number of iterations has been performed, <math>m = M</math>, then exit. Otherwise, set <math>m := m + 1</math> and continue from step 2.</p>
---

global. This section is a discussion of the interpretation of approximate results. An example concludes the section.

The purpose of the lattice training algorithm is to find lattices with the lowest possible value of the normalized second moment  $G$ , for a given dimension  $d$ . The exact computation of  $G$  for a general lattice involves the determination of every vertex, edge, 2-dimensional face, etc., of the Voronoi region [41]. The complexity of this computation grows dramatically with the dimension, so it is practically feasible only for lattices of moderate dimension. As a less complex alternative,  $G$  can be estimated through Monte Carlo integration of (24). This method, proposed by Conway and Sloane in [36], is the one we use in this paper. We also follow their nomenclature in presenting estimates of  $G$  on the form  $\hat{G} \pm 2\hat{\sigma}$ , where  $\hat{\sigma}$  is an estimate of the standard deviation of  $\hat{G}$ .

When the lattice training algorithm exits, it has converged to the vicinity of a local minimum. Thus, the training algorithm does not directly point out exact local minima  $\mathbf{f}^*$ ; it terminates anywhere inside a small region around  $\mathbf{f}^*$ . All  $\mathbf{f}$ 's inside the region represent the same minimum, and to find this (exact) minimum, we need some kind of "rounding" process. The rounding, which takes place when the training is complete, is guided by the following rule.

*Postulate 1:* If two lattices represent the same local minimum, the one with most symmetry is the more accurate representative.

The postulate is empirically motivated. Nature favors symmetry. In the past, every lattice that has shown good quantization performance has also possessed a high degree of symmetry, while on the other hand, the (unrounded) lattices generated by the training algorithm have minimum symmetry (that is, reflection in the origin and nothing else). Zamir and Feder [34] show that the optimal lattice quantization noise is *white*, which means that if a random vector  $\mathbf{e}$ , uniformly distributed in the optimal Voronoi region, is projected onto an arbitrary line, the obtained random variable has the same variance regardless of the orientation of the line. This property certainly supports the notion of symmetric Voronoi regions. There is a practical reason to encourage symmetry as well: search time. For many lattices, the symmetrical structure has been exploited in the development of very efficient search algorithms [42].

In the comparison of lattices, it is important to remember the possibilities of basis change and rotation. As discussed in Section I-C, equivalent lattices can have generator matrices that look quite different from each other, which is why the identification of a lattice requires some manual efforts.

Suppose that the output of the training algorithm is a generator matrix  $\mathbf{B}_1$ . To identify the lattice, we need to find matrices  $\mathbf{W}$  and  $\mathbf{Q}$ , and a scale factor given by  $V_2$ , such that  $\mathbf{B}_2$  in (17) gets a suitable form, preferably one that has been described in the literature, if this is possible. The first thing that we do is to estimate the normalized second moment  $G$ , which is independent of both  $\mathbf{W}$  and  $\mathbf{Q}$ , and also of the scaling. If the estimate agrees with a value that we have seen for another lattice in the same dimension, in the literature or in our experiments, it is likely that the two lattices are equivalent. To prove it, we study the innermost *shell* of the lattice, that is, the set of nonzero lattice points being closest to  $\mathbf{0}$ . This set of points, which is independent of  $\mathbf{W}$  but not  $\mathbf{Q}$ , can be computed by a modified closest point algorithm [39]. The radius of the shell (which equals twice the *packing radius*) and the number of points in it (the *kissing number*) are two  $\mathbf{Q}$ -independent lattice parameters, so they should be equal for equivalent lattices (if  $V_2 = V_1$ ). If they are, we complete the proof by selecting a subset of the shell for both lattices and rotating the two subsets into each other, thus obtaining  $\mathbf{Q}$ .

The following example demonstrates how a 5-dimensional lattice was identified through suitable choices of the  $\mathbf{W}$  and  $\mathbf{Q}$  matrices. The example also illustrates how we employ postulate 1 to round the resulting matrix to a more symmetrical one. The method and the magnitude of rounding in this example are representative for the experiments in the next section, where other lattices obtained by the training algorithm are identified.

*Example 1:* For  $d = 5$ , one run of the lattice training algorithm gave the following generator matrix:

$$\mathbf{B}_1 = \begin{bmatrix} 1.285 & 0.000 & 0.000 & 0.000 & 0.000 \\ -0.518 & 1.025 & 0.000 & 0.000 & 0.000 \\ -0.255 & 0.517 & 1.149 & 0.000 & 0.000 \\ -0.514 & -0.261 & -0.579 & 0.811 & 0.000 \\ 0.513 & 0.263 & -0.572 & -0.003 & 0.815 \end{bmatrix}$$

and the normalized second moment  $G$  was estimated to  $0.075624 \pm 0.000010$ . Direct inspection of the generator matrix does not immediately suggest any symmetries. However, we observe that the best 5-dimensional lattice currently known,  $D_5^*$ , has a normalized second moment of  $G = 2^{-48/5} \cdot 2641/45 \approx 0.075625$  [43], which falls well within the interval estimated for  $\mathbf{B}_1$ . Hence, the  $D_5^*$  lattice is the hypothesis that we try to verify. Employing the strategy outlined above, we create another generator matrix through (17) with a basis change given by

$$\mathbf{W} = \begin{bmatrix} 0 & -1 & 0 & 0 & 0 \\ 1 & 0 & 1 & 1 & 0 \\ 0 & 0 & 0 & -1 & 0 \\ 0 & 0 & 0 & 0 & 1 \\ 1 & 0 & 0 & 0 & 0 \end{bmatrix},$$

a rotation given by

$$\mathbf{Q} = \begin{bmatrix} 0.449011 & 0.448323 & 0.447087 & 0.446851 & 0.444785 \\ -0.893513 & 0.224658 & 0.226453 & 0.227533 & 0.219344 \\ 0.001054 & 0.496921 & 0.500431 & -0.500429 & -0.502203 \\ -0.001532 & 0.708240 & -0.705966 & -0.002575 & -0.000121 \\ 0.004514 & -0.001350 & -0.003817 & 0.705774 & -0.708411 \end{bmatrix},$$

and a scaling of  $V_2/V_1 = 0.5$ . The new generator matrix,

$$\mathbf{B}_2 = \left(\frac{V_2}{V_1}\right)^{1/d} \mathbf{W}\mathbf{B}_1\mathbf{Q} = \begin{bmatrix} 1.000 & 0.002 & -0.000 & -0.001 & 0.005 \\ 0.002 & 0.999 & 0.002 & 0.001 & -0.001 \\ -0.000 & 0.002 & 1.002 & 0.001 & -0.004 \\ -0.001 & 0.001 & 0.001 & 1.002 & -0.003 \\ 0.502 & 0.501 & 0.500 & 0.500 & 0.498 \end{bmatrix},$$

specifies a lattice that is equivalent to  $\mathbf{B}_1$ . The structure underlying this matrix is clearly visible, and postulate 1 allows us to create a

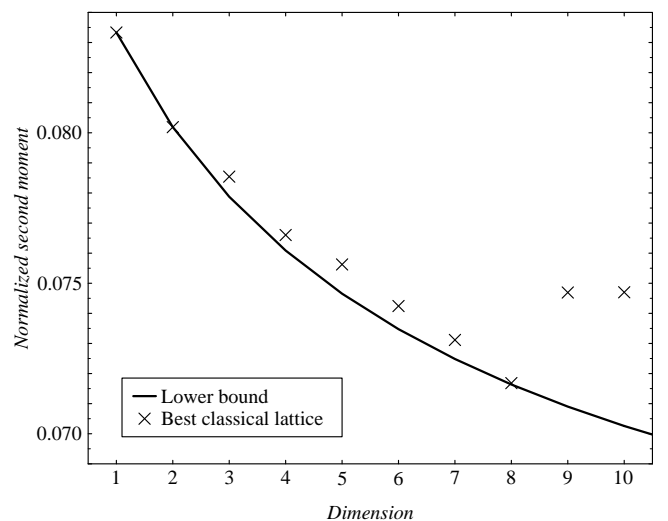


**Fig. 2.** The lowest normalized second moments previously known, in dimensions 1–10. This diagram is supplemented with our results in subsequent figures.

more accurate representation of the found minimum by rounding the elements:

$$\mathbf{B} = \begin{bmatrix} 1 & 0 & 0 & 0 & 0 \\ 0 & 1 & 0 & 0 & 0 \\ 0 & 0 & 1 & 0 & 0 \\ 0 & 0 & 0 & 1 & 0 \\ 1/2 & 1/2 & 1/2 & 1/2 & 1/2 \end{bmatrix},$$

which is indeed a generator matrix of the very symmetrical  $D_5^*$  lattice (A.3).  $\square$

### III. EXPERIMENTS

The work presented in this paper was inspired by the need for better lattices for quantization. As discussed in Section I, the performance of a lattice quantizer is, under some circumstances, characterized by the normalized second moment of the lattice,  $G$ . Fig. 2 summarizes the best classical lattices [43–46, 33, 47] along with Conway and Sloane’s conjectured lower bound [44]. With “classical” we mean lattices for which the normalized second moment has been reported previously. The figure hints a potential for improvement, especially in 9 and 10 dimensions. 10-dimensional quantization has received a lot of attention in speech coding [48, 49], where suboptimal structures such as split VQ and multistage VQ have been much employed. A good 10-dimensional lattice might provide an attractive alternative in this application.

In Section III-A, the results obtained through lattice training are presented. When the dimension  $d$  is 9 or 10, we find lattices with normalized second moments considerably lower than the values previously known for these dimensions. If the new lattices are indeed optimal, they disprove a famous conjecture by Conway and Sloane. The structure of the new lattices draws our attention to a class of nonlattice tessellations, which is examined in Section III-B. We report tessellations that are better than all previously studied tessellations, including lattices, in 7 and 9 dimensions. We tried to focus the section on the results of the training algorithm, without expanding the work into an essay on lattice theory. Hence, some theoretical background and definitions are left to references.

#### A. The Best Lattices Found

There is no theoretical limitation on the number of dimensions that the lattice training algorithm can handle, only a practical one. The algorithm, in its present form, typically requires 2 hours in 3 dimensions, 4 hours in 10, and 25 hours in 20. With other training parameters, time can, of course, be bought to the price of accuracy. To evaluate the algorithm, especially to assess its ability to converge into local minima with low normalized second moments  $G$ , we considered it important to run the algorithm several times in each dimension, and identify each output lattice through the methodology of Section II-C, in a manner similar to example 1. This required some manual work on each lattice, the amount of which ranged from seconds to hours for the identification of a single lattice.

The considerations above led to the following experiment setup. The training algorithm was run 10 times in each dimension from 2 to 10, and the trained lattices were identified. Most of this section is devoted to results from this experiment. To study some further features of the algorithm, we also designed 100 3-dimensional lattices and one 20-dimensional one.

During training, we regularly output an estimate of  $G$ . Except during the very first iterations, we have never observed any sudden change, and in all tested cases, the algorithm had converged well before the decreasing step size  $\epsilon_m$  caused the training to cease. This observation suggests that no numerical problems significantly disturb the algorithm. Especially, the algorithm manages to avoid the problem of “sensitive” lattices (see Section II-B).

In Table II, the 10 lattices obtained in dimensions 2–10 are listed, grouped according to which local minimum they represent. Normalized second moments  $G$  were estimated for one (randomly selected) member of each group. Most of the groups represent one of the “classical” lattices, among which the most notable are  $\mathbb{Z}^d$ ,  $A_d$ , and  $A_d^*$  for  $d \geq 1$ ;  $D_d$  and  $D_d^*$  for  $d \geq 3$ ; and  $E_d$  and  $E_d^*$  for  $6 \leq d \leq 8$ . They are all defined in the appendix and their properties (normalized second moment, etc.) can be found in [2, chs. 4 and 21]. A few groups do not represent any known and named lattice; these lattices are characterized below. For comparison, the previously best

TABLE II  
THE LATTICES OBTAINED BY THE TRAINING ALGORITHM, GROUPED ACCORDING TO LOCAL MINIMA. INTERVALS ARE GIVEN ON THE FORM  $\hat{G} \pm 2\hat{\sigma}$ , SEE SECTION II-C.

$d$	Trained lattices				Previously best known		Lower bound
	Number of local minima	Hits in each minimum	$G$	Name of minimum	$G$	Name	$G$
2	1	10	$0.080180 \pm 0.000010$	$A_2$	0.080188	$A_2$	0.080188
3	1	10	$0.078540 \pm 0.000010$	$A_3^*$	0.078543	$A_3^*$	0.077875
4	2	9	$0.076602 \pm 0.000010$	$D_4^*$	0.076603	$D_4$	0.076087
		1	$0.077551 \pm 0.000010$	$A_4^*$			
5	2	9	$0.075624 \pm 0.000010$	$D_5^*$	0.075625	$D_5^*$	0.074654
		1	$0.075796 \pm 0.000010$	—			
6	2	7	$0.074240 \pm 0.000010$	$E_6^*$	0.074244	$E_6^*$	0.073475
		3	$0.074342 \pm 0.000010$	$E_6$			
7	2	9	$0.073121 \pm 0.000010$	$E_7^*$	0.073116	$E_7^*$	0.072484
		1	$0.073234 \pm 0.000010$	$E_7$			
8	1	10	$0.071681 \pm 0.000010$	$E_8$	0.071682	$E_8$	0.071636
9	3	8	$0.071626 \pm 0.000002$	—	0.074693	$D_9^*$	0.070902
		1	$0.071634 \pm 0.000002$	—			
		1	$0.071640 \pm 0.000003$	—			
10	1	10	$0.070814 \pm 0.000010$	$D_{10}^*$	0.074701	$D_{10}^*$	0.070258

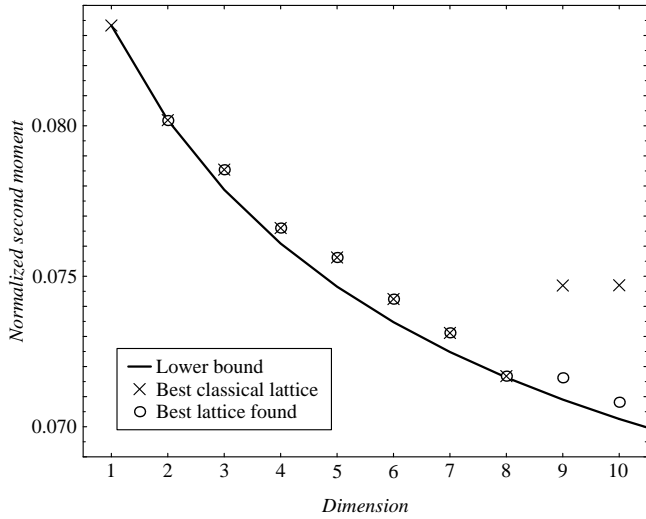


Fig. 3. A comparison between classical lattices and the principal minima given by the training algorithm.

known  $G$  values<sup>11</sup> and Conway and Sloane’s lower bound<sup>12</sup> are included in the table.

The 10 runs for each dimension turned out to converge into just a few different local minima; more than three local minima were not found for any dimension. Of these minima, one, called the *principal minimum* for a given  $d$ , always got significantly more hits than the others. It can be seen in Table II that in all dimensions, the principal minimum turned out to be equivalent to the best known  $d$ -dimensional lattice—or better! In none of the studied dimensions, our lattice training algorithm failed to reach a performance that has been attained through other design methods. In dimensions 9 and 10, we found lattices that have not been considered for quantization before. Both these cases are discussed in detail below. In dimensions 2–8, the principal minima were equivalent to best known results, which lends confidence to our training algorithm as well as to previous investigations. We do not claim that the principal minimum found by the lattice training algorithm is always the global minimum, but we have not yet seen a counterexample.

Fig. 3 summarizes the results obtained by lattice training, in relation to the previously known results of Fig. 2. Lattice training carries the normalized second moment much closer to the bound for  $d = 9$  and 10. In 10 dimensions, the gain over the best classical lattice,  $D_{10}^*$ , is 0.23 dB, a gain that (18) indicates can be interpreted as the SNR difference between corresponding lattice quantizers.

We now comment on the results in each dimension; first we give a brief summary of dimensions from 2 to 8, then a more detailed presentation of dimensions 9 and 10, which is where our lattice results improve on previous knowledge. For  $d = 2$  and 3, all trials converged to the same local minimum,  $A_2$  and  $A_3^*$ . For  $d = 4$  and 5, we found two local minima, of which the principal ones ( $D_4$  and  $D_5^*$ ) were reached in 9 out of 10 attempts. The suboptimal local minima are  $A_4^*$  and an unnamed 5-dimensional sublattice of  $D_6^*$ .<sup>13</sup> For  $d = 6$  and 7, the principal minimum is  $E_d^*$ , and  $E_d$  is a secondary minimum. For  $d = 8$ , the only local minimum found is

<sup>11</sup> Among the “best known” lattices, only the ones in dimensions 1–3 have been proven optimal.

<sup>12</sup> The values were computed using a series expansion of the recursive integral equation in [44].

<sup>13</sup> The 5-dimensional locally optimal lattice can be obtained as the intersection of  $D_5^*$  and a hyperplane perpendicular to the vector  $(1, 1, 1, 1, 1)^T$ . This specification of the new lattice is analogous to the definition of  $E_7$  as a sublattice of  $D_8^*$ , see the appendix.

$E_8$ , which is known as a very good and very symmetrical lattice [44].

Before proceeding to the lattices found in dimensions 9 and 10, we pause to make an observation on the less frequent local minima in Table II. Since some local minima only received one hit in 10 attempts, there may well exist other lattices that are also locally optimal, even though none of the 10 runs arrived there. If we wish to estimate the exact number of local minima in a given dimension, 10 trials are apparently insufficient; if, on the other hand, we are more concerned with finding the one global optimum in each dimension, the trend of better local minima getting more hits, as the table indicates, is encouraging. As an example of a thorough search for local minima, we executed the algorithm 100 times in 3 dimensions. All of them converged to  $A_3^*$  as expected; Barnes and Sloane have shown that this is the only 3-dimensional local minimum [2, p. 60]. Especially, the *face-centered cubic lattice*,  $A_3$ , was never reached. Its  $G$  is only slightly higher than that of  $A_3^*$ , but it is not even locally optimal.

Nine-dimensional lattices are special. The lattices we reached are more irregular than the ones in other dimensions, and none of them were found in the literature. Moreover, they do not appear to be *integer lattices* [2, p. 47] for any scaling, which makes them unique amongst the presently best known lattices. While confusing at first, this irregularity was to some extent explained when we studied nonlattice tessellation (see Section III-B). It turned out that there is a 9-dimensional nonlattice tessellation (yes, a highly regular tessellation!) that is considerably better than all known lattices. If the optimal tessellation for  $d = 9$  is not a lattice at all, then the irregular lattices that we observe may be attempts by the training algorithm to approximate the nonlattice structure within a lattice constraint.

The generator matrix of the 9-dimensional principal minimum is

$$\begin{bmatrix} 2 & 0 & 0 & 0 & 0 & 0 & 0 & 0 & 0 \\ 1 & 1 & 0 & 0 & 0 & 0 & 0 & 0 & 0 \\ 1 & 0 & 1 & 0 & 0 & 0 & 0 & 0 & 0 \\ 1 & 0 & 0 & 1 & 0 & 0 & 0 & 0 & 0 \\ 1 & 0 & 0 & 0 & 1 & 0 & 0 & 0 & 0 \\ 1 & 0 & 0 & 0 & 0 & 1 & 0 & 0 & 0 \\ 1 & 0 & 0 & 0 & 0 & 0 & 1 & 0 & 0 \\ 1 & 0 & 0 & 0 & 0 & 0 & 0 & 1 & 0 \\ 1/2 & 1/2 & 1/2 & 1/2 & 1/2 & 1/2 & 1/2 & 1/2 & 0.573 \end{bmatrix} \quad (31)$$

and the normalized second moment of the lattice was estimated to  $0.071622 \pm 0.000003$ . In (31), we have interpreted the output of the algorithm according to postulate 1, but for this lattice, the postulate does not give exact values of all matrix elements. One element, 0.573, was left unrounded. We will explain later why no value can be replaced for 0.573 to increase the symmetry of the lattice.

Since postulate 1 yields exact values of all but one element of the generator matrix of this locally optimal lattice, a single-variate optimization algorithm can be formulated to increase the accuracy of this one variable. We modified the lattice training algorithm of Section II for this purpose. The lattice structure was constrained to (31) with an unknown variable substituted for the lower right element. A derivative similar to (30) was calculated and the algorithm was run to optimize the single variable. The theory by Zamir and Feder on the whiteness of lattice quantization noise (see Section II-C) shows that this optimization problem has a unique minimum. The result, based on 100 runs of the single-variate training algorithm, was  $0.57321 \pm 0.00014$ , where the interval is again given on the form

$\pm 2\hat{\sigma}$ , using an estimate  $\hat{\sigma}$  of the standard deviation. Hence, the three decimals in (31) can be considered significant.<sup>14</sup>

The matrix (31) generates a peculiar lattice, in which the lattice points lie closer together along the  $d$ th coordinate than along the others. This follows from the fact that the nonzero lattice points closest to the origin are  $\pm(0,0,\dots,0,1.146)$ .<sup>15</sup> Just these two points; for example,  $(1.146,0,0,\dots,0)$  is not a lattice point. The distance to the two closest points is 1.146; in other directions, the distance to any lattice point is 2 or greater. Hence, the Voronoi region of this lattice is flat. It is tempting to conclude that the lattice therefore must have a relatively high normalized second moment  $G$ , since this measure characterizes how round the Voronoi region is (see Section I-B), but the conclusion is severely wrong. A lower  $G$  is not known among 9-dimensional lattices. This lattice apparently compensates its weird 9th coordinate with being extremely round in the first 8 dimensions. The projection of the lattice orthogonal to  $(0,0,\dots,0,1.146)$  is  $D_8^+$ , better known as  $E_8$ , whose Voronoi region is very round, as mentioned above. The geometry of the 9th coordinate also explains why symmetry arguments will not suffice to identify the local minimum represented by (31) completely. To use an analogy, a cylinder cannot be made more symmetrical by changing its height.

The two suboptimal local minima that the algorithm converged into one time each for  $d=9$  display similar irregularities. One of them reminds much of (31) above, in that it has a pair of vectors being significantly shorter than any other lattice vector, and the projection orthogonal to them is  $E_8$ . The last local optimum has two pairs of extra short vectors, and the projection orthogonal to both of them is  $E_7^*$ .

The obtained 10-dimensional lattices, finally, are all equivalent to the lattice generated by

$$\begin{pmatrix} 2 & 0 & 0 & 0 & 0 & 0 & 0 & 0 & 0 & 0 \\ 1 & 1 & 0 & 0 & 0 & 0 & 0 & 0 & 0 & 0 \\ 1 & 0 & 1 & 0 & 0 & 0 & 0 & 0 & 0 & 0 \\ 1 & 0 & 0 & 1 & 0 & 0 & 0 & 0 & 0 & 0 \\ 1 & 0 & 0 & 0 & 1 & 0 & 0 & 0 & 0 & 0 \\ 1 & 0 & 0 & 0 & 0 & 1 & 0 & 0 & 0 & 0 \\ 1 & 0 & 0 & 0 & 0 & 0 & 1 & 0 & 0 & 0 \\ 1 & 0 & 0 & 0 & 0 & 0 & 0 & 1 & 0 & 0 \\ 1 & 0 & 0 & 0 & 0 & 0 & 0 & 0 & 1 & 0 \\ 1/2 & 1/2 & 1/2 & 1/2 & 1/2 & 1/2 & 1/2 & 1/2 & 1/2 & 1/2 \end{pmatrix}. \quad (32)$$

This lattice is well known, it is called  $D_{10}^+$ , but it has, to our knowledge, not been considered for quantization earlier. Its normalized second moment lies very close to the lower bound; we estimated  $\hat{G} = 0.070813 \pm 0.000003$ . More on the  $D^+$  family, including a very fast search method, is discussed in the next section.

There is a famous conjecture regarding the relation between optimal lattices for “quantization” and “packing.”<sup>16</sup> It is based on the observation that the best known  $d$ -dimensional lattices for the two purposes were always each other’s duals. In 1982, Conway and Sloane conjectured that this duality would be true for the optimal lattices in any dimension [43]. They supported the conjecture in [36] but later expressed some doubts [2, p. 62]. Forney has devoted a

<sup>14</sup> Kenneth Zeger points in a personal communication out that  $(4 + \sqrt{3})/10 = 0.57321$ . Whether this is the exact value or a coincidence is an open question.

<sup>15</sup> To see that these points belong to the lattice, use the construction  $\mathbf{B}^T \mathbf{u}$  with  $\mathbf{u} = \mp(-3, 1, 1, \dots, 1, -2)$ .

<sup>16</sup> In the lattice literature, the *quantization* problem is to minimize  $G$ , and the *packing* problem [2, Ch. 1] is to maximize

$$\delta = \frac{1}{V} \left( \inf_{\mathbf{x} \in \Omega} \|\mathbf{x}\| \right)^d$$

TABLE III  
LATTICES THAT CHALLENGE CONWAY AND SLOANE’S  
CONJECTURE. SHADED CELLS DENOTE BEST KNOWN VALUES  
IN THEIR DIMENSION.

Lattice	$G$	$\delta$ of dual
(31)	0.071622 $\pm$ 0.000003	0.02857 $\pm$ 0.00002
$\Lambda_9^*$	0.071769 $\pm$ 0.000006	$1/16\sqrt{2} \approx 0.04419$
$D_{10}^+$	0.070813 $\pm$ 0.000003	$1/32 = 0.03125$
$\Lambda_{10}^*$	0.071339 $\pm$ 0.000009	$1/16\sqrt{3} \approx 0.03608$

paper to the duality conjecture, suggesting that it, although not true in its present form, might be a first-order approximation of a yet unknown relation [47]. However, no counterexample has been presented to date, which motivates an investigation of our 9- and 10-dimensional discoveries in this context.

The best known lattices for packing in 9 and 10 dimensions are called  $\Lambda_9$  and  $\Lambda_{10}$ , respectively [2, chs. 1 and 6]. The best known lattices for quantization are now given by (31) and (32), the latter being  $D_{10}^+$ . In Table III, we show that our new lattices have a lower  $G$  than  $\Lambda_9^*$  and  $\Lambda_{10}^*$ , thus showing that  $\Lambda_9^*$  and  $\Lambda_{10}^*$  are not optimal, as the conjecture would imply. We also show that the duals of the new lattices are not optimal packings, which, if it were true, would have been a second way to satisfy the conjecture.

Our new lattice results thus strongly indicate that the conjecture is false, but they do not prove it. A proof would be complete the day one of the four shaded values in Table III would be proved optimal. For now, we have to be content with a “counter-conjecture”:  $d=9$  is the lowest dimension for which the optimal lattices for quantization and packing are *not* duals.

The present study ends with  $d=10$ , but the algorithm is able to design lattices in considerably higher dimensions than this. The only thing that limits the number of dimensions is, as far as we have found, the available time. As an example, a 20-dimensional lattice was designed. It took 25 hours, and the normalized second moment of the resulting lattice was estimated to  $0.067594 \pm 0.000005$ . The lower bound for  $d=20$  is 0.066457.

### B. The Best Tessellations Found

In the study of the trained lattices, we were struck by the similarities between the best found lattices in 8 and 10 dimensions. In this section, we generalize the pattern and discover very good nonlattice tessellations in 7 and 9 dimensions. Traditionally, the study of tessellation for quantization applications has been heavily dominated by lattices, see, e.g., [2, p. 61]. This is, to our knowledge, the first time that nonlattice tessellations have shown any competitive performance in relation to lattices.

Compare (32) and (41): the pattern is obvious. On the other hand, the best found lattice in 9 dimensions (31) is different, not very much, but still significantly. The key to this mystery lies in the  $D^+$  family. It is defined as the union of  $D_d$  and a translation of  $D_d$  [2, pp. 46 and 119]:

$$D_d^+ = D_d \cup (D_d + (1/2, \dots, 1/2)^T) \quad (33)$$

where  $D_d$  is defined in the appendix. When  $d$  is even,  $D_d^+$  is a lattice, whereas for odd values of  $d$ ,  $D_d^+$  is a nonlattice tessellation. We will return to the geometrical properties of  $D_d^+$ , and the peculiar 9th dimension later in the section. For now, we turn to the main point of interest, namely, the normalized second moment.

Fig. 4 shows the results in dimensions from 2 to 10. For comparison, the figure includes the conjectured lower bound [44] and the best known lattices, including the new results from the previous

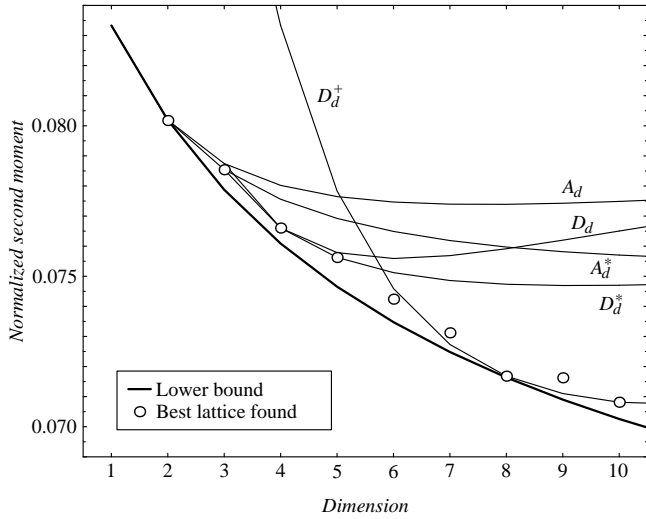


**Fig. 4.** The performance of the  $D_d^+$  tessellation, versus lattices and the lower bound. Note the improvement in 7 and 9 dimensions.

section. The performances of the lattices  $A_d$ ,  $A_d^*$ ,  $D_d$ , and  $D_d^*$  [43] are also shown.  $D_d^+$  gives significantly lower normalized second moments than these four lattice families for  $d \geq 6$ ; the curve for  $D_d^+$  indeed passes through the best lattices in 8 and 10 dimensions, as expected. In 7 and 9 dimensions, however, the best known lattices are inferior to  $D_d^+$ , which performs considerably closer to the lower bound. That the best lattices have higher normalized second moments than other tessellations in certain dimensions has never before been observed.

In Table IV, the results in dimensions from 7 to 10 are summarized in terms of normalized second moment. The new contributions of this paper are indicated by a shaded background.

Consider Fig. 4 again and observe  $G$  for the best lattices, that is, study the pattern formed by the circles. Without too much imagination, the pattern can be described as somewhat zigzag: lattices are in general worse for odd dimensions than for even, compared with the lower bound. This property can, to some extent, be explained by the relation between lattices and nonlattice tessellations. To put it simple, good tessellations are more often lattices in even dimensions than in odd. This observation motivates a closer look upon the geometry of  $D_d^+$ .

It is not hard to show that when  $d$  is even,  $D_d^+$  is a lattice, with the generator matrix

$$\mathbf{B} = \begin{bmatrix} 2 & 0 & 0 & \cdots & 0 \\ 1 & 1 & 0 & \cdots & 0 \\ 1 & 0 & 1 & \cdots & 0 \\ \vdots & \vdots & \vdots & \ddots & \vdots \\ 1/2 & 1/2 & 1/2 & \cdots & 1/2 \end{bmatrix}. \quad (34)$$

The situation is more complicated when  $d$  is odd. To begin with, (34) does *not* generate  $D_d^+$ . Instead, it generates a peculiar lattice,

TABLE IV  
THE BEST KNOWN NORMALIZED SECOND MOMENT  $G$  FOR  
LATTICES AND TESSELLATIONS IN DIMENSIONS 7–10.  
SHADED CELLS DENOTE NEW RESULTS.

$d$	Best known lattice	Best known tessellation	Lower bound
7	0.073116	0.072734 ± 0.000003	0.072484
8	0.071682	0.071682	0.071636
9	0.071622 ± 0.000003	0.071103 ± 0.000003	0.070902
10	0.070813 ± 0.000003	0.070813 ± 0.000003	0.070258

which has many characteristics in common with the best found 9-dimensional lattice (31) discussed above. E. g.,  $\pm(0,0,\dots,0,1)$  are lattice points, so the lattice points lie closer together along the  $d$ th coordinate than along the others. For  $d=9$ , (34) generates  $\Lambda_9^*$ , which was discussed in connection with Table III.

So what is the generator matrix of  $D_d^+$  for odd values of  $d$ ? The answer is that there is none. As mentioned,  $D_d^+$  is not a lattice when  $d$  is odd. However, it is still a tessellation, because all its Voronoi regions are congruent. Half of them are upside-down (more precisely, reflected in a point), which disqualifies the tessellation from being a lattice. In a lattice, all Voronoi regions are translations of each other, without scaling, rotation, or reflection, see Section I-C.

Conway and Sloane [2, p. 120] summarize some parameters of the tessellation  $D_d^+$ . We conclude this section by adding two facts to their list, without further comments. The *covering radius* is  $R = \sqrt{3}/2$  ( $d=3$ ), 1 ( $4 \leq d \leq 8$ ),  $\sqrt{d}/8$  (even  $d \geq 8$ ), or  $\sqrt{2d-1}/4$  (odd  $d \geq 8$ ). For even  $d$ , the lattice  $D_d^+$  is *geometrically self-dual* [2, p. xix]: the dual is equivalent to the lattice itself.

#### IV. SUMMARY AND CONCLUSIONS

We have investigated the concept of designing lattices with low normalized second moments through numerical optimization. The main results of the paper can be concluded in the following points.

- We develop an iterative algorithm, which initially has the ability to escape shallow local minima, but the ability decreases with training time.
- The optimization problem has relatively few local minima. Of the local minima, our experiments tend to converge into the better ones.
- Numerically generated lattices can yield exact lattices by symmetry arguments.
- In dimensions 2–8, we rediscover the lattices that have previously been reported as best known.
- In dimension 9, a new lattice (31) is discovered, which is considerably better than any lattice previously known. It has an uncommon structure for locally optimal lattices.
- In dimension 10, a significant improvement can be attained by employing  $D_{10}^+$  instead of the lattices that have been considered before.
- Experiments suggest that the method is applicable to optimization in considerably higher dimensions than 10.
- The new lattices suggest that the famous duality conjecture by Conway and Sloane may be false.
- We show that the  $D_d^+$  tessellation performs better than any known lattice tessellation in dimensions 7 and 9. This is the first time that lattices do not hold all second moment world records for tessellations.

As a graphical summary, we conclude this paper with Fig. 5, which presents our values (circles and dots) compared with what was previously known.

#### APPENDIX: THE CLASSICAL LATTICES

In this appendix, the lattices  $\mathbb{Z}^d$ ,  $A_d$ ,  $D_d$ , and  $E_d$  are briefly defined. A much more thorough treatise on their structure and properties is found in [2, ch. 4].

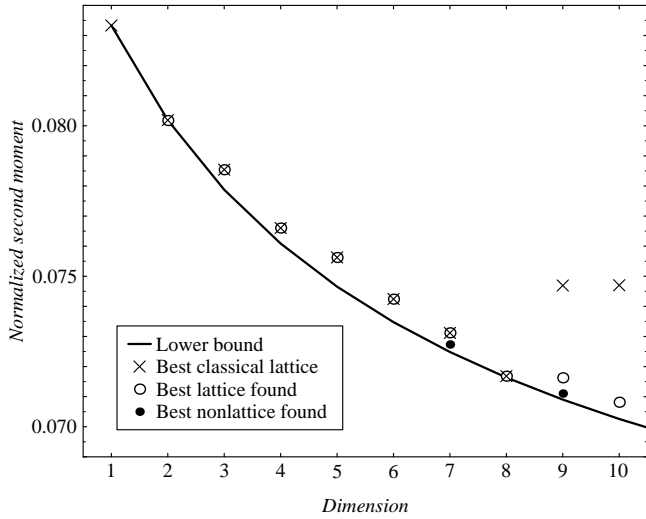


Fig. 5. A comparison between classical lattices and the lattices and tessellations found through training.

The *cubic lattice*  $\mathbb{Z}^d$  is the Cartesian product of  $d$  1-dimensional lattices. The generator matrix depends, as discussed in Section I-C, on rotation and choice of basis vectors. One generator matrix for  $\mathbb{Z}^d$  is the  $d \times d$  identity matrix. The lattice is its own dual.

The lattice  $A_d$  can be defined as a sublattice of the cubic lattice:  $A_d$  consists of the points of  $\mathbb{Z}^{d+1}$  that lie on a hyperplane orthogonal to  $(1, 1, \dots, 1)^T$ . A rotated version of  $A_d$  is generated by the matrix<sup>17</sup>

$$\begin{bmatrix} \alpha & 1 & \dots & 1 \\ 1 & \alpha & \dots & 1 \\ \vdots & \vdots & \ddots & \vdots \\ 1 & 1 & \dots & \alpha \end{bmatrix} \quad (35)$$

where  $\alpha = \sqrt{d+1} + 2$ .  $A_2$  is the hexagonal lattice, see Fig. 1. One choice of a generator matrix of the dual  $A_d^*$  is (35) with  $\alpha = \sqrt{d+1} - d$ .

The lattice  $D_d$  is defined for  $d \geq 3$ . It consists of every second point in  $\mathbb{Z}^d$ , namely, those points whose coordinate sum is even. A generator matrix is

$$\begin{bmatrix} 2 & 0 & 0 & \dots & 0 \\ 1 & 1 & 0 & \dots & 0 \\ 1 & 0 & 1 & \dots & 0 \\ \vdots & \vdots & \vdots & \ddots & \vdots \\ 1 & 0 & 0 & \dots & 1 \end{bmatrix}. \quad (36)$$

Its dual,  $D_d^*$  has the generator matrix

$$\begin{bmatrix} 1 & 0 & \dots & 0 & 0 \\ 0 & 1 & \dots & 0 & 0 \\ \vdots & \vdots & \ddots & \vdots & \vdots \\ 0 & 0 & \dots & 1 & 0 \\ 1/2 & 1/2 & \dots & 1/2 & 1/2 \end{bmatrix}. \quad (37)$$

The  $E_d$  family is defined for  $d=6, 7$ , and 8 only.  $E_6$  is a sublattice of  $A_7^*$ . With  $A_7^*$  generated by (35),  $E_6$  is the lattice being orthogonal to any of the basis vectors of  $A_7^*$ . A generator matrix for  $E_6$  and its dual is

$$\begin{bmatrix} 1 & 0 & 0 & 0 & 0 & \alpha \\ 0 & 1 & 0 & 0 & 0 & \alpha \\ 0 & 0 & 1 & 0 & 0 & \alpha \\ 0 & 0 & 0 & 1 & 0 & \alpha \\ 0 & 0 & 0 & 0 & 1 & \alpha \\ 1/2 & 1/2 & 1/2 & 1/2 & 1/2 & 3\alpha/2 \end{bmatrix} \quad (38)$$

with  $\alpha = \sqrt{3}$  for  $E_6$  and  $\alpha = 1/\sqrt{3}$  for  $E_6^*$ .  $E_7$  is the sublattice of  $D_8^*$  (37) being orthogonal to  $(1, 1, \dots, 1)^T$ . As a generator matrices for  $E_7$ , we can use

$$\begin{bmatrix} 2 & 0 & 0 & 0 & 0 & 0 & 0 \\ 0 & 2 & 0 & 0 & 0 & 0 & 0 \\ 0 & 0 & 2 & 0 & 0 & 0 & 0 \\ 0 & 0 & 0 & 2 & 0 & 0 & 0 \\ 1 & 1 & 1 & 0 & 1 & 0 & 0 \\ 0 & 1 & 1 & 1 & 0 & 1 & 0 \\ 0 & 0 & 1 & 1 & 1 & 0 & 1 \end{bmatrix} \quad (39)$$

and for  $E_7^*$ ,

$$\begin{bmatrix} 2 & 0 & 0 & 0 & 0 & 0 & 0 \\ 0 & 2 & 0 & 0 & 0 & 0 & 0 \\ 0 & 0 & 2 & 0 & 0 & 0 & 0 \\ 1 & 1 & 0 & 1 & 0 & 0 & 0 \\ 0 & 1 & 1 & 0 & 1 & 0 & 0 \\ 0 & 0 & 1 & 1 & 0 & 1 & 0 \\ 0 & 0 & 0 & 1 & 1 & 0 & 1 \end{bmatrix}. \quad (40)$$

$E_8$ , finally, is equivalent to  $D_8^+$ , see Section III-B. The lattice, which is also equivalent to its dual  $E_8^*$ , can be generated by the matrix

$$\begin{bmatrix} 2 & 0 & 0 & 0 & 0 & 0 & 0 & 0 \\ 1 & 1 & 0 & 0 & 0 & 0 & 0 & 0 \\ 1 & 0 & 1 & 0 & 0 & 0 & 0 & 0 \\ 1 & 0 & 0 & 1 & 0 & 0 & 0 & 0 \\ 1 & 0 & 0 & 0 & 1 & 0 & 0 & 0 \\ 1 & 0 & 0 & 0 & 0 & 1 & 0 & 0 \\ 1 & 0 & 0 & 0 & 0 & 0 & 1 & 0 \\ 1/2 & 1/2 & 1/2 & 1/2 & 1/2 & 1/2 & 1/2 & 1/2 \end{bmatrix}. \quad (41)$$

## REFERENCES

- [1] T. Eriksson and E. Agrell, "Lattice-Based Quantization, Part II," Tech. Report 18, Dept. of Information Theory, Chalmers Univ. of Technology, Göteborg, Sweden, 1996.
- [2] J. H. Conway and N. J. A. Sloane, *Sphere Packings, Lattices and Groups*, 2nd ed. New York, NY: Springer-Verlag, 1993.
- [3] S. P. Lloyd, "Least squares quantization in PCM," *IEEE Trans. Inform. Theory*, vol. IT-28, no. 2, pp. 129–137, Mar. 1982.
- [4] Y. Linde, A. Buzo, and R. M. Gray, "An algorithm for vector quantizer design," *IEEE Trans. Commun.*, vol. COM-28, no. 1, pp. 84–95, Jan. 1980.
- [5] T. Kohonen, *Self-Organization and Associative Memory*, 2nd ed. Berlin, Germany: Springer-Verlag, 1988.
- [6] J. K. Flanagan, D. R. Morrell, R. L. Frost, C. J. Read, and B. E. Nelson, "Vector quantization codebook generation using simulated annealing," in *Proc. IEEE International Conference on Acoustics, Speech, and Signal Processing*, vol. 3, pp. 1759–1762, Glasgow, Scotland, U.K., May 1989.
- [7] A. Gersho, "Asymptotically optimal block quantization," *IEEE Trans. Inform. Theory*, vol. IT-25, no. 4, pp. 373–380, July 1979.
- [8] T. Linder and K. Zeger, "Asymptotic entropy-constrained performance of tessellating and universal randomized lattice quantization," *IEEE Trans. Inform. Theory*, vol. 40, no. 2, pp. 575–579, Mar. 1994.
- [9] A. Gersho, "On the structure of vector quantizers," *IEEE Trans. Inform. Theory*, vol. IT-28, no. 2, pp. 157–166, Mar. 1982.
- [10] H. Cohn, *A Second Course in Number Theory*. New York, NY: John Wiley & Sons, 1962.

<sup>17</sup> For consistency, we give square generator matrices for all lattices, which is why some of our definitions may appear unfamiliar. Especially in literature with focus on theory rather than application, it is common to present the lattices  $A_d$ ,  $E_6$ ,  $E_7$ , and their duals using nonsquare generator matrices.

- [11] G. L. Nemhauser and L. A. Wolsey, *Integer and Combinatorial Optimization*. New York, NY: John Wiley & Sons, 1988.
- [12] N. S. Jayant and P. Noll, *Digital Coding of Waveforms: Principles and Applications to Speech and Video*. Englewood Cliffs, NJ: Prentice-Hall, 1984.
- [13] T. Berger, *Rate Distortion Theory. A Mathematical Basis for Data Compression*. Englewood Cliffs, NJ: Prentice-Hall, 1971.
- [14] T. R. Fischer, "Geometric source coding and vector quantization," *IEEE Trans. Inform. Theory*, vol. 35, no. 1, pp. 137–145, Jan. 1989.
- [15] C. E. Shannon, "Communication in the presence of noise," *Proceedings of the I.R.E.*, vol. 37, no. 1, pp. 10–21, Jan. 1949.
- [16] T. R. Fischer, "A pyramid vector quantizer," *IEEE Trans. Inform. Theory*, vol. IT-32, no. 4, pp. 568–583, July 1986.
- [17] C. Lamblin, J. P. Adoul, D. Massaloux, and S. Morissette, "Fast CELP coding based on the Barnes-Wall lattice in 16 dimensions," in *Proc. IEEE International Conference on Acoustics, Speech, and Signal Processing*, vol. 1, pp. 61–64, Glasgow, Scotland, U.K., May 1989.
- [18] M. Xie and J.-P. Adoul, "Embedded algebraic vector quantizers (EAVQ) with application to wideband speech coding," in *Proc. IEEE International Conference on Acoustics, Speech, and Signal Processing*, vol. 1, pp. 240–243, Atlanta, GA, May 1996.
- [19] D. G. Jeong and J. D. Gibson, "Lattice vector quantization for image coding," in *Proc. IEEE International Conference on Acoustics, Speech, and Signal Processing*, vol. 3, pp. 1743–1746, Glasgow, Scotland, U.K., May 1989.
- [20] D. G. Jeong and J. D. Gibson, "Uniform and piecewise uniform lattice vector quantization for memoryless Gaussian and Laplacian sources," *IEEE Trans. Inform. Theory*, vol. 39, no. 3, pp. 786–804, May 1993.
- [21] P. W. Moo and D. L. Neuhoff, "An asymptotic analysis of fixed-rate lattice vector quantization," in *Proc. IEEE International Symposium on Information Theory and Its Applications*, vol. 1, pp. 409–412, Victoria, British Columbia, Canada, Sept. 1996.
- [22] F. Kuhlmann and J. A. Bucklew, "Piecewise uniform vector quantizers," *IEEE Trans. Inform. Theory*, vol. 34, no. 5, pp. 1259–1263, Sept. 1988.
- [23] P. F. Swaszek, "Unrestricted multistage vector quantizers," *IEEE Trans. Inform. Theory*, vol. 38, no. 3, pp. 1169–1174, May 1992.
- [24] T. Eriksson, "Multistage vector quantization with dynamic bit allocation," in *Signal Processing VII: Theories and Applications*, vol. 1, M. J. J. Holt, C. F. N. Cowan, P. M. Grant, and W. A. Sandham, Eds., pp. 383–386, *Proc. EUSIPCO*, Edinburgh, Scotland, U.K., Sept. 1994.
- [25] J. Pan and T. R. Fischer, "Two-stage vector quantization—lattice vector quantization," *IEEE Trans. Inform. Theory*, vol. 41, no. 1, pp. 155–163, Jan. 1995.
- [26] J. A. Bucklew, "Companding and random quantization in several dimensions," *IEEE Trans. Inform. Theory*, vol. IT-27, no. 2, pp. 207–211, Mar. 1981.
- [27] J. A. Bucklew, "A note on optimal multidimensional companders," *IEEE Trans. Inform. Theory*, vol. IT-29, no. 2, p. 279, Mar. 1983.
- [28] M. Antonini, M. Barlaud, and T. Gaidon, "Adaptive entropy constrained lattice vector quantization for multiresolution image coding," in *Proceedings of SPIE*, vol. 1818, pt. 2, P. Maragos, Ed., pp. 441–457, *Proc. Visual Communications and Image Processing*, Boston, MA, Nov. 1992.
- [29] R. M. Gray, *Source Coding Theory*. Boston, MA: Kluwer Academic Publishers, 1990.
- [30] A. Gersho and R. M. Gray, *Vector Quantization and Signal Compression*. Boston, MA: Kluwer Academic Publishers, 1992.
- [31] M. Antonini, M. Barlaud, and P. Mathieu, "Image coding using lattice vector quantization of wavelet coefficients," in *Proc. IEEE International Conference on Acoustics, Speech, and Signal Processing*, vol. 4, pp. 2273–2276, Toronto, Ontario, Canada, May 1991.
- [32] Z. Mohd-Yusof and T. R. Fischer, "An entropy-coded lattice vector quantizer for transform and subband image coding," *IEEE Transactions on Image Processing*, vol. 5, no. 2, pp. 289–298, Feb. 1996.
- [33] T. D. Lookabaugh and R. M. Gray, "High-resolution quantization theory and the vector quantizer advantage," *IEEE Trans. Inform. Theory*, vol. 35, no. 5, pp. 1020–1033, Sept. 1989.
- [34] R. Zamir and M. Feder, "On lattice quantization noise," *IEEE Trans. Inform. Theory*, vol. 42, no. 4, pp. 1152–1159, July 1996.
- [35] L. T. Wille, "New binary covering codes obtained by simulated annealing," *IEEE Trans. Inform. Theory*, vol. 42, no. 1, pp. 300–302, Jan. 1996.
- [36] J. H. Conway and N. J. A. Sloane, "On the Voronoi regions of certain lattices," *SIAM Journal on Algebraic and Discrete Methods*, vol. 5, no. 3, pp. 294–305, Sept. 1984.
- [37] A. K. Lenstra, H. W. Lenstra, Jr., and L. Lovász, "Factoring polynomials with rational coefficients," *Mathematische Annalen*, vol. 261, pp. 515–534, 1982.
- [38] R. Kannan, "Improved algorithms for integer programming and related lattice problems," in *Proc. Annual ACM Symposium on Theory of Computing*, pp. 193–206, Boston, MA, Apr. 1983.
- [39] E. Agrell and T. Eriksson, unpublished work, 1996. **updated below**
- [40] L. Babai, "On Lovász' lattice reduction and the nearest lattice point problem," *Combinatorica*, vol. 6, no. 1, pp. 1–13, 1986.
- [41] E. Viterbo and E. Biglieri, "Computing the Voronoi cell of a lattice: the diamond-cutting algorithm," *IEEE Trans. Inform. Theory*, vol. 42, no. 1, pp. 161–171, Jan. 1996.
- [42] J. H. Conway and N. J. A. Sloane, "Fast quantizing and decoding algorithms for lattice quantizers and codes," *IEEE Trans. Inform. Theory*, vol. IT-28, no. 2, pp. 227–232, Mar. 1982.
- [43] J. H. Conway and N. J. A. Sloane, "Voronoi regions of lattices, second moments of polytopes, and quantization," *IEEE Trans. Inform. Theory*, vol. IT-28, no. 2, pp. 211–226, Mar. 1982.
- [44] J. H. Conway and N. J. A. Sloane, "A lower bound on the average error of vector quantizers," *IEEE Trans. Inform. Theory*, vol. IT-31, no. 1, pp. 106–109, Jan. 1985.
- [45] J. Makhoul, S. Roucos, and H. Gish, "Vector quantization in speech coding," *Proc. IEEE*, vol. 73, no. 11, pp. 1551–1588, Nov. 1985.
- [46] J. D. Gibson and K. Sayood, "Lattice quantization," in *Advances in Electronics and Electron Physics*, vol. 72, P. W. Hawkes and B. Kazan, Eds. Boston, MA: Academic Press, pp. 259–330, 1988.
- [47] G. D. Forney, Jr., "On the duality of coding and quantization," in *DIMACS Series in Discrete Mathematics and Theoretical Computer Science, Vol. 14: Coding and Quantization*, R. Calderbank, G. D. Forney, Jr., and N. Moayeri, Eds. Providence, RI: American Mathematical Society, pp. 1–14, 1993.
- [48] K. K. Paliwal and B. S. Atal, "Efficient vector quantization of LPC parameters at 24 bits/frame," in *Proc. IEEE International Conference on Acoustics, Speech, and Signal Processing*, vol. 1, pp. 661–664, Toronto, Ontario, Canada, May 1991.
- [49] P. Hedelin, "Single stage spectral quantization at 20 bits," in *Proc. IEEE International Conference on Acoustics, Speech, and Signal Processing*, vol. 1, pp. 525–528, Adelaide, Australia, Apr. 1994.
- [39] E. Agrell, T. Eriksson, A. Vardy, and K. Zeger, "Closest point search in lattices," *IEEE Trans. Inform. Theory*, vol. 48, no. 8, pp. 2201–2214, Aug. 2002.